Journal of Sound and Vibration (2003) **259**(3), 525–539
doi:10.1006/jsvi.2002.5335, available online at http://www.idealibrary.com on IDEAL®

VIBRATION ANALYSIS OF NON-CIRCULAR CURVED PANELS BY THE DIFFERENTIAL QUADRATURE METHOD

S. T. Choi

Institute of Aeronautics and Astronautics, National Cheng Kung University, Tainan, Taiwan 70101, *Republic of China. E-mail: choi@mail.ncku.edu.tw*

AND

Y. T. Chou

Department of Mechanical Engineering, Yung Ta Institute of Technology, Lin Loc, Ping Tung, Taiwan 909, *Republic of China*

(*Received* 22 *January* 2002, *and in final form* 2 *April* 2002)

Free-vibration characteristics of cantilever non-circular curved panels are analyzed by using the differential quadrature method (DQM) in this paper. The equations of motion of a curved panel are based on the Love's hypothesis and are expressed in an orthogonal curvilinear co-ordinate system. By applying the differential quadrature formulation and the proposed modified relationships for specified boundary conditions, the free-vibration equations of motion of the curved panel are transformed to a set of algebraic equations. Natural frequencies of a cantilever flat plate and a circular curved panel are obtained for verifying the applicability of the present approach. Good convergent trend and accuracy are observed. Effects of shallowness, thickness and aspect ratios on the natural frequencies of a cantilever curved panel are also investigated. Furthermore, natural frequencies of parabolic curved panels are obtained. In all cases studied, the efficiency and convenience of the DQM are illustrated.

1. INTRODUCTION

For high structural performance of advanced machinery or engineering structures, vibration characteristics of shells have drawn attention for studying. Love postulated the first approximation of the classical thin shell theory to investigate the behavior of the small-amplitude free vibration for a thin elastic shell [1]. Olson and Lindberg [2] obtained the natural frequencies of uniform and tapered fan blades with various boundary conditions by the finite element method, and some experimental results were also presented to verify the numerical results. Leissa [3] summarized the works of the vibration aspects of thin shells before the 1970s. Leissa *et al*. [4, 5] and Wang [6] solved the vibration problems of cantilever and rotating blades by the Ritz method. Leissa and Ewing [7] compared the vibration frequencies of turbomachinery blades between beam and shell theories. The deviation of the fundamental frequency between these two models is not significant for a blade with a large aspect ratio; however, the discrepancy is obvious for a blade with a small aspect ratio. Lim and Liew [8] analyzed the flexural vibration of a cylindrical shell with rectangular planform by the pb-2 Ritz method. In a more recent survey, Liew *et al*. [9] reviewed the development of research in vibration of shallow shells.

0022-460X/02/$35.00

The validity and range of applicability for three kinds of shell theory, Kirchhoff–Love, first order and higher order, are examined.

Characteristics of engineering problems are of complex geometry and loading of different types. Analytical solutions of these problems usually cannot be obtained easily. With the ever-growing advancement of faster computers, numerical procedures are alternative for obtaining solutions to these problems. A variety of numerical methods are available today for engineering analysis, such as: finite difference method, finite element method, and boundary element method. These methods provide accurate results when sufficiently fine meshes are used. However, this may consume longer computation time. The differential quadrature method (DQM), which transforms governing equations of differential form to matrix form by using weighting matrices, is a computationally efficient method. The DQM requires small amount of computer capacity and is able to provide accurate results. The DQM first introduced by Bellman and Casti [10] is an efficient numerical method for rapid solutions of linear and non-linear partial differential equations. Bert *et al.* [11–13] applied this method to structural problems involving fourth order partial differential equations. Since then, many researchers have applied this method in many engineering areas. Sherbourne and Pandey [14] analyzed buckling of beams and composite plates. Shu and Richards [15] solved the two-dimensional incompressible Navier–Stokes equations. Gutierrez and Laura [16] solved the Helmholtz equation in a parallelogrammic domain with mixed boundary conditions. In 1996, Bert and Malik [17] reviewed the development of DQM in computational mechanics. Three-dimensional elasticity solutions for free vibrations of rectangular plates were obtained by Malik and Bert [18], and Liew and Teo [19]. Choi *et al.* [20] studied the dynamic behavior of spinning Timoshenko beams. Choi and Chou [21] investigated elastically supported turbomachinery blades by the modified differential quadrature method.

There are, however, some drawbacks in the original DQM. For problems involving fourth or higher order differential equations for which two or more boundary conditions need to be specified at each boundary point, numerical error is induced by using the direct deletion or δ-point method in the original DQM since boundary conditions are not exactly satisfied. To overcome this problem, different approaches had been proposed [22–27]. Wang and Bert [22] and Bert *et al.* [23] incorporated the boundary conditions in the weighting coefficient matrix in the context of beam and plate vibration problems. Malik and Bert [24] presented a detailed methodology for implementing multiple boundary conditions in DQM. However, there were still some limitations in their approach. It could not yield results of any dependable accuracy for rectangular plates having two or more adjacent free edges. Shu and Du [25, 26] proposed an approach that directly couples the boundary conditions with the governing equations, and obtained accurate results for plate without free corners. However, for plate configuration with at least one free corner, a new grid point distribution has to be used for obtaining more accurate results. Choi and Chou [21, 28] proposed a new approach in using the DQM. Modified relationships were proposed and a new formulation process was presented in this approach, which is different from that used by Wang and Bert [22] and Bert *et al.* [23]. High efficiency and accuracy have been illustrated in vibrational analysis of beams and turbomachinery blades by using this new approach.

In this paper, the dynamic characteristics of cantilever curved panels are studied by using the DQM and by following the approach used by Choi and Chou [21]. Modified relationships are used for specified boundary conditions and are integrated with the governing equations of motion. Natural frequencies of a cantilever flat plate and a circular curved panel are obtained for verifying the applicability of the present approach. Effects of shallowness, thickness and aspect ratios on the natural frequencies of a cantilever curved panel are also investigated. Furthermore, natural frequencies of parabolic curved panels are obtained.

2. DQM FOR SHELL PROBLEMS

The basic concept of the DQM is that the derivative of a function, with respect to a space variable at a given sampling point, is approximated as a weighted linear sum of the function values at all of the sampling points in the domain of that variable. Differential equations are then transformed to a set of algebraic equations for time-independent problems and a set of ordinary differential equations in time for initial/boundary-value problems.

The configuration of a thin non-circular curved panel is shown in Figure 1. The orthogonal curvilinear co-ordinate system x–s–z is used. The principal radius of curvature at the mid-surface ($z = 0$) of the panel is denoted by $R_s(s)$. In general, a panel is meshed by N_x and N_s sampling points in the x and s directions respectively. The total number of sampling points is $N_x \times N_s$ in the domain of the panel. The co-ordinates of sampling points are chosen as [15]

$$x_i = \frac{a}{2}(1 - \cos[(i-1)\pi/(N_x - 1)]), \quad i = 1, 2, \ldots, N_x, \tag{1a}$$

$$s_j = \frac{b}{2}(1 - \cos[(j-1)\pi/(N_s - 1)]), \quad j = 1, 2, \ldots, N_s, \tag{1b}$$

where a and b are the lengths of the panel in the x and s directions respectively. The sampling points for a curved panel are distributed as in Figure 2.

For a two-dimensional problem, two weighting matrices corresponding to differentiation with respect to x and to s are represented in the DQ formulation as, respectively,

$$\frac{\partial f(x_i, s_j)}{\partial x} = \sum_{m=1}^{N_x} c_{im}^{(x)} f(x_m, s_j) \quad \text{for} \quad \begin{array}{l} i = 1, 2, \ldots, N_x, \\ j = 1, 2, \ldots, N_s, \end{array} \tag{2a}$$

$$\frac{\partial f(x_i, s_j)}{\partial s} = \sum_{m=1}^{N_s} c_{jm}^{(s)} f(x_i, s_m) \quad \text{for} \quad \begin{array}{l} i = 1, 2, \ldots, N_x, \\ j = 1, 2, \ldots, N_s, \end{array} \tag{2b}$$

where $c_{im}^{(x)}$ and $c_{jm}^{(s)}$ are weighting matrices, and are N_x and N_s square matrices respectively. For deriving the weighting matrices, the value of the function $f(x, s)$ can be approximated

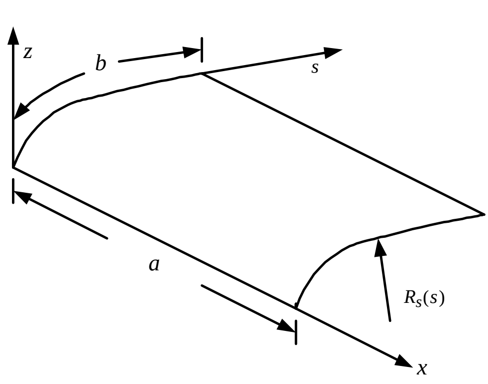

Figure 1. Configuration of a non-circular curved panel with a rectangular planform.

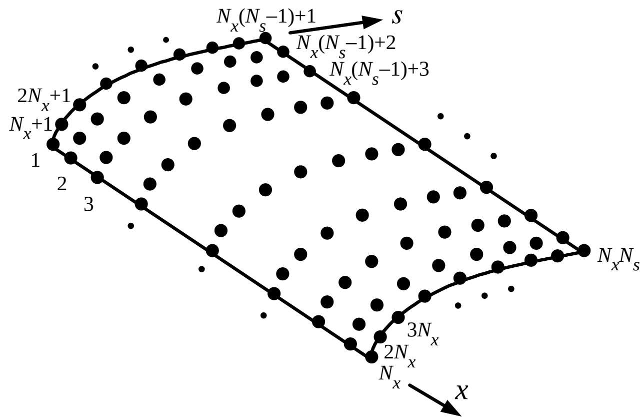

Figure 2. Distribution and numbering of sampling points for a non-circular curved panel.

by the polynomial $\Phi_{kl}(x, s)$ with the following form:

$$\Phi_{kl}(x, s) = g_k(x) \cdot h_l(s), \tag{3}$$

where $g_k(x)$ and $h_l(s)$ are the one-dimensional Lagrangian interpolation functions corresponding to x and s directions, respectively, and they are represented as [15]

$$g_k(x) = \frac{M(x)}{(x - x_k)M^*(x_k)}, \quad k = 1, 2, \ldots, N_x, \tag{4a}$$

$$h_l(s) = \frac{L(s)}{(s - s_l)L^*(s_l)}, \quad l = 1, 2, \ldots, N_s, \tag{4b}$$

where

$$M(x) = \prod_{m=1}^{N_x}(x - x_m), \qquad M^*(x_k) = \prod_{\substack{m=1 \\ m \neq k}}^{N_x}(x_k - x_m), \quad k = 1, 2, \ldots, N_x,$$

and

$$L(s) = \prod_{m=1}^{N_s}(s - s_m), \qquad L^*(s_l) = \prod_{\substack{m=1 \\ m \neq l}}^{N_s}(s_l - s_m), \quad l = 1, 2, \cdots, N_s.$$

By introducing the test functions $\Phi_{kl}(x, s)$ of equation (3) into equations (2a,b) for $f(x, s)$, the weighting matrices can be obtained as [15]

$$c_{im}^{(x)} = \frac{M^*(x_i)}{(x_i - x_m)M^*(x_m)}, \quad i \neq m \quad \text{and} \quad c_{ii}^{(x)} = -\sum_{\substack{m=1 \\ m \neq i}}^{N_x} c_{im}^{(x)}, \quad i, m = 1, 2, \ldots, N_x$$

and

$$c_{jm}^{(s)} = \frac{L^*(s_j)}{(s_j - s_m)L^*(s_m)}, \quad j \neq m \quad \text{and} \quad c_{jj}^{(s)} = -\sum_{\substack{m=1 \\ m \neq j}}^{N_s} c_{jm}^{(s)}, \quad j, m = 1, 2, \ldots, N_s.$$

As described above, the function values $f(x_i, s_j)$ form an $N_x \times N_s$ matrix and for matrix manipulation, it has to be rearranged as a column vector

$$\tilde{f} = \left\{f_{1,1}, f_{2,1}, \cdots, f_{N_x,1}, f_{1,2}, f_{2,2}, \ldots, f_{N_x,2}, \ldots, f_{1,N_s}, f_{2,N_s}, \ldots, f_{N_x,N_s}\right\}^{\mathrm{T}},$$

where $f_{i,j} = f(x_i, s_j)$. For this purpose, the weighting matrices $c_{im}^{(x)}$ and $c_{jm}^{(s)}$ are rearranged to the new weighting matrices $\bar{W}_X$ and $\bar{W}_S$ as

$$\bar{W}_X = \begin{bmatrix} \left[c_{im}^{(x)}\right] & [0] & \cdots & [0] \\ [0] & \left[c_{im}^{(x)}\right] & \cdots & [0] \\ \vdots & \vdots & \ddots & \vdots \\ [0] & [0] & \cdots & \left[c_{im}^{(x)}\right] \end{bmatrix}, \quad i, m = 1, 2, \ldots, N_x$$

and

$$\bar{W}_S = \begin{bmatrix} c_{11}^{(s)}[I] & c_{12}^{(s)}[I] & \cdots & c_{1N_s}^{(s)}[I] \\ c_{21}^{(s)}[I] & c_{22}^{(s)}[I] & \cdots & c_{1N_s}^{(s)}[I] \\ \vdots & \vdots & \ddots & \vdots \\ c_{N_s1}^{(s)}[I] & c_{N_s2}^{(s)}[I] & \cdots & c_{N_sN_s}^{(s)}[I] \end{bmatrix},$$

where $[I]$ is an identity matrix of dimension N_x, and $\bar{W}_X$ and $\bar{W}_S$ are both square matrices of dimension $N_x{\cdot}N_s$. It is seen that there are many zeros in the new weighting matrices. Using the technique for sparse matrices, the storage requirement in the computational process is reduced. By using the new weighting matrices, the DQ formulation and the modified relationships described below can be easily incorporated.

The DQ formulation of two-dimensional problems can be rewritten in terms of the new weighting matrices $\bar{W}_X$ and $\bar{W}_S$ and the rearranged function vector $\tilde{f}$ as

$$\frac{\partial \tilde{f}}{\partial x} = \bar{W}_X \tilde{f} \quad \text{and} \quad \frac{\partial \tilde{f}}{\partial s} = \bar{W}_S \tilde{f}. \tag{5}$$

2.1. MODIFIED RELATIONSHIPS

In this paper, curved panels with classical boundary conditions are considered. Modified relationships are deduced by considering boundary conditions. As an example, the relationship between the displacement w and the slope along the x-axis, θ_x, is

$$\theta_x = -\frac{\partial w}{\partial x}.$$

In the discretized domain, the modified relationship [21] for the above expression is written as

$$\tilde{\theta}_x = -\bar{W}_X \bar{\boldsymbol{B}}^{(w)} \tilde{w}, \tag{6}$$

where $\bar{\boldsymbol{B}}^{(w)}$ is the modified matrix corresponding to the boundary conditions of the displacement w. The modified matrix $\bar{\boldsymbol{B}}^{(w)}$ is obtained from an identity matrix of dimension $N_x{\cdot}N_s$ by setting zero to elements corresponding to locations of null boundary value of w. Modified relationships for other variables are derived in a similar manner.

For a cantilever curved panel that is clamped at the edge $x = 0$ and is free at the other three edges, the displacements are zero at the sampling points along the edge $x = 0$, i.e.,

$$w_i = 0, \quad \text{where } i = 1,\ N_x + 1,\ 2N_x + 1, \ldots, (N_s - 1)N_x + 1.$$

These i's correspond to the sampling point numbers at the edge $x = 0$ as shown in Figure 2. Then for this case, the modified matrix $\bar{B}^{(w)}$ is obtained from an identity matrix by setting the following diagonal element to zeros:

$$B_{ii}^{(w)} = 0, \quad \text{where } i = 1,\ N_x + 1,\ 2N_x + 1, \ldots, (N_s - 1)N_x + 1.$$

3. PROBLEM FORMULATION

By following the Kirchhoff–Love hypothesis, the displacement field of the curved panel shown in Figure 1 is assumed as [1]

$$U(x, s, z) = u(x, s) + z\beta_x(x, s), \tag{7a}$$

$$V(x, s, z) = v(x, s) + z\beta_s(x, s), \qquad W(x, s, z) = w(x, s), \tag{7b, c}$$

where u, v and w are displacements of the mid-surface of the panel; z is the distance measured from the mid-surface; β_x and β_s are the angles of rotation for x and s directions, respectively. If the shear deformation is neglected, β_x and β_s are represented as

$$\beta_x = -\frac{\partial w}{\partial x},$$

$$\beta_s = -\frac{\partial w}{\partial s} + \frac{v}{R_s},$$

Substituting equations (7a–c) into strain–displacement relations referred to an orthogonal curvilinear co-ordinate system, one obtains the strain components ε_{xx}, ε_{ss} and ε_{xs} as

$$\varepsilon_{xx} = \overset{\circ}{\varepsilon}_{xx} + z\kappa_{xx}, \qquad \varepsilon_{ss} = \overset{\circ}{\varepsilon}_{ss} + z\kappa_{ss}, \qquad \varepsilon_{xs} = \overset{\circ}{\varepsilon}_{xs} + z\kappa_{xs}, \tag{8a – c}$$

where $\overset{\circ}{\varepsilon}_{xx}$, $\overset{\circ}{\varepsilon}_{ss}$ and $\varepsilon_{xs}{}^{\circ}$ are the strains of the mid-surface of the panel; κ_{xx}, κ_{ss}, and κ_{xs} are the curvatures. They are given as

$$\varepsilon_{xx}{}^{\circ} = \frac{\partial u}{\partial x}, \quad \varepsilon_{ss}{}^{\circ} = \frac{\partial v}{\partial s} + \frac{w}{R_s}, \quad \varepsilon_{xs}{}^{\circ} = \frac{\partial u}{\partial s} + \frac{\partial v}{\partial x},$$

$$\kappa_{xx} = \frac{\partial \beta_x}{\partial x}, \quad \kappa_{ss} = \frac{\partial \beta_s}{\partial s}, \quad \kappa_{xs} = \frac{\partial \beta_x}{\partial s} + \frac{\partial \beta_s}{\partial x}.$$

Stresses acting on a shell element of isotropic material are given as

$$\sigma_{xx} = \frac{E}{1 - v^2}(\varepsilon_{xx} + v\varepsilon_{ss}), \qquad \sigma_{ss} = \frac{E}{1 - v^2}(\varepsilon_{ss} + v\varepsilon_{xx}), \tag{9a, b}$$

$$\sigma_{xs} = G\varepsilon_{xs}, \tag{9c}$$

where v is Poisson's ratio, E and G are Young's and shear moduli respectively.

By integrating all stresses acting on a shell element whose dimensions are infinitesimal in the x and s directions, the membrane forces N_{xx}, N_{ss} and N_{xs} are given as

$$N_{xx} = K(\varepsilon_{xx}{}^{\circ} + v\varepsilon_{ss}{}^{\circ}), \qquad N_{ss} = K(\varepsilon_{ss}{}^{\circ} + v\varepsilon_{xx}{}^{\circ}), \tag{10a, b}$$

$$N_{xs} = N_{sx} = \frac{K(1 - v)}{2}\varepsilon_{xs}{}^{\circ} \tag{10c}$$

and the bending moments M_{xx}, M_{ss} and M_{xs} as

$$M_{xx} = D(\kappa_{xx} + v\kappa_{ss}), \qquad M_{ss} = D(\kappa_{ss} + v\kappa_{xx}), \tag{11a, b}$$

$$M_{xs} = M_{sx} = \frac{D(1-\nu)}{2}\kappa_{xs}, \tag{11c}$$

where the membrane and bending stiffnesses are, respectively, $K = Eh(x,s)/(1-\nu^2)$ and $D = Eh^3(x,s)/[12(1-\nu^2)]$, and $h(x,s)$ is the thickness of the panel.

By using Hamilton's principle, the governing equations of motion of the curved panel can be derived as [1]

$$\frac{\partial N_{xx}}{\partial x} + \frac{\partial N_{xs}}{\partial s} = \rho h\ddot{u}, \tag{12a}$$

$$\frac{\partial N_{sx}}{\partial x} + \frac{\partial N_{ss}}{\partial s} + \frac{Q_{sz}}{R_s} = \rho h\ddot{v}, \tag{12b}$$

$$\frac{\partial Q_{xz}}{\partial x} + \frac{\partial Q_{sz}}{\partial s} + \frac{N_{ss}}{R_s} = \rho h\ddot{w}, \tag{12c}$$

where ρ is the material density, and Q_{xz} and Q_{sz} are transverse shear forces and are defined by

$$Q_{xz} = \frac{\partial M_{xx}}{\partial x} + \frac{\partial M_{sx}}{\partial s}, \tag{13a}$$

$$Q_{sz} = \frac{\partial M_{xs}}{\partial x} + \frac{\partial M_{ss}}{\partial s}. \tag{13b}$$

The DQ formulation can be easily introduced into equations (12) and (13) by incorporating modified relationships. From equations (13), we have

$$\tilde{Q}_{xz} = \bar{W}_X\bar{B}^{(M_{xx})}\tilde{M}_{xx} + \bar{W}_S\bar{B}^{(M_{xs})}\tilde{M}_{xs}, \tag{14a}$$

$$\tilde{Q}_{sz} = \bar{W}_X\bar{B}^{(M_{xs})}\tilde{M}_{xs} + \bar{W}_S\bar{B}^{(M_{ss})}\tilde{M}_{ss}. \tag{14b}$$

By assuming free vibration with frequency ω for the curved panel and using equations (14), equations (12) are transformed to algebraic equations as

$$\bar{W}_X\bar{B}^{(N_{xx})}\tilde{N}_{xx} + \bar{W}_S\bar{B}^{(N_{xs})}\tilde{N}_{xs} = -\rho\omega^2\bar{H}\tilde{u}, \tag{15a}$$

$$\begin{aligned} &\bar{W}_X\bar{B}^{(N_{xs})}\tilde{N}_{xs} + \bar{W}_S\bar{B}^{(N_{ss})}\tilde{N}_{ss} \\ &+ \bar{R}_s^{-1}\left[\bar{W}_X\bar{B}^{(M_{xs})}\tilde{M}_{xs} + \bar{W}_S\bar{B}^{(M_{ss})}\tilde{M}_{ss}\right] = -\rho\omega^2\bar{H}\tilde{v}, \end{aligned} \tag{15b}$$

$$\begin{aligned} &\bar{W}_X\left[\bar{W}_X\bar{B}^{(M_{xx})}\tilde{M}_{xx} + \bar{W}_S\bar{B}^{(M_{xs})}\tilde{M}_{xs}\right] \\ &+ \bar{W}_S\left[\bar{W}_X\bar{B}^{(M_{xs})}\tilde{M}_{xs} + \bar{W}_S\bar{B}^{(M_{ss})}\tilde{M}_{ss}\right] + \bar{R}_s^{-1}\tilde{N}_{ss} = -\rho\omega^2\bar{H}\tilde{w}, \end{aligned} \tag{15c}$$

where $\bar{W}_X$ and $\bar{W}_S$ are the rearranged weighting matrices with respect to x- and s-co-ordinates, respectively; $\bar{H}$ and $\bar{R}_s$ are diagonal matrices corresponding to varying thickness and curvature of the panel respectively. $\bar{B}^{(\bullet)}$ are modified matrices that are determined from boundary conditions and are similar to $\bar{B}^{(w)}$ described in equation (6). The same formulation process is also applied to equations (7)–(11). The final system equations can be combined and represented as

$$[K_G]\{\tilde{U}\} = \omega^2[M_G]\{\tilde{U}\}, \tag{16}$$

where

$$[K_G] = \begin{bmatrix} \bar{K}_{11} & \bar{K}_{12} & \bar{K}_{13} \\ \bar{K}_{21} & \bar{K}_{22} & \bar{K}_{23} \\ \bar{K}_{31} & \bar{K}_{32} & \bar{K}_{33} \end{bmatrix},$$

$$[M_G] = \begin{bmatrix} \bar{M}_{11} & 0 & 0 \\ 0 & \bar{M}_{22} & 0 \\ 0 & 0 & \bar{M}_{33} \end{bmatrix}$$

and

$$\{\tilde{U}\} = \{\tilde{u} \;\; \tilde{v} \;\; \tilde{w}\}^{\mathrm{T}}.$$

The sub-matrices of $[K_G]$ and $[M_G]$ are given in Appendix A.

3.1. BOUNDARY CONDITIONS

In this study, curved panels with clamped and free edges are considered. For a clamped edge along the edge $x = 0$ or $x = a$, the boundary conditions are $u = v = w = \beta_x = 0$.

For a free edge, two kinds of Kirchhoff's boundary conditions are written as

(1) First kind of Kirchhoff's conditions:

$$V_{xz} = Q_{xz} + \frac{\partial M_{xs}}{\partial s}, \quad V_{sz} = Q_{sz} + \frac{\partial M_{sx}}{\partial x}. \tag{17a, b}$$

(2) Second kind of Kirchhoff's conditions:

$$T_{xs} = N_{xs} + \frac{M_{xs}}{R_s}, \quad T_{sx} = N_{sx}. \tag{18a, b}$$

The boundary conditions for a C–F–F–F non-circular curved panel are

$$x = 0 : u = v = w = \beta_x = 0,$$

$$x = a : N_{xx} = T_{xs} = M_{xx} = V_{xz} = 0,$$

$$s = 0 \text{ and } s = b : \quad N_{ss} = T_{sx} = M_{ss} = V_{sz} = 0.$$

It should be noticed that when two adjacent edges of a panel are free, there is an additional boundary condition for the corner force. It requires that the corner force $F_c = 2M_{xs} = 0$. The modified matrices $\bar{B}^{(\bullet)}$ of a C–F–F–F panel are deduced from identity matrices by setting zeros to the following elements corresponding to zero boundary value:

$$B_{ii}^{(u)} = B_{ii}^{(v)} = B_{ii}^{(w)} = B_{ii}^{(\beta_x)} = 0 \quad \text{for } i = 1,\, N_x + 1,\, 2N_x + 1, \ldots, (N_S - 1)N_x + 1,$$

$$B_{ii}^{(N_{ss})} = B_{ii}^{(T_{xs})} = B_{ii}^{(M_{ss})} = B_{ii}^{(V_{sz})} = 0 \quad \text{for } i = 1,\, 2, \ldots, N_x,$$

$$B_{ii}^{(N_{xx})} = B_{ii}^{(T_{sx})} = B_{ii}^{(M_{xx})} = B_{ii}^{(V_{xz})} = 0 \quad \text{for } i = N_x,\, 2N_x, 3N_x, \ldots, N_x N_s,$$

$$B_{ii}^{(N_{ss})} = B_{ii}^{(T_{xs})} = B_{ii}^{(M_{ss})} = B_{ii}^{(V_{sz})} = 0 \quad \text{for } i = (N_s - 1)N_x + 1,\, (N_s - 1)N_x + 2, \ldots, N_x N_s$$

and

$$B_{ii}^{(M_{xs})} = 0 \quad \text{for } i = N_x \text{ and } N_x N_s.$$

By introducing the modified matrices and solving the eigenvalue problem of equation (16), the natural frequencies of a cantilever non-circular curved panel can be obtained.

4. RESULTS AND DISCUSSION

4.1. STUDY 1: CONVERGENCE AND COMPARISON

The first six non-dimensional frequencies of a square cantilever flat plate are obtained by using the present approach with different grids of sampling points. Results are shown in Table 1 together with the analytical solutions for the same plate obtained by Leissa [29] using the Rayleigh–Ritz method. It can be seen that as the number of sampling points increases, the non-dimensional frequency converges to values which are slightly less than the corresponding ones obtained by Leissa. This is reasonable because Leissa's results are upper bounds of natural frequencies. Good convergence trends of the present results are observed in this table. Results with satisfactory accuracy are obtained by using a grid of $9*9$ sampling points, and the present results agree with the data by Leissa [29] to within 1%. A $9*9$ grid is thus adopted for results presented in this section. It is noted that accurate and convergent results could not be obtained by the conventional DQM used by Malik and Bert [24].

A cantilever (C–F–F–F) circular curved panel with a uniform thickness is studied. The material properties and the dimensions of the panel used in the present computation are

$$E = 200\,\text{GPa},\ \rho = 7860\,\text{kg/m}^3,\ v = 0{\cdot}3,$$

$$R_S = 0{\cdot}6096\,\text{m},\ h = 0{\cdot}003\,\text{m},\ a = b = 0{\cdot}3048\,\text{m}.$$

Natural frequencies of the panel obtained by the present approach are shown in Table 2, in which the results obtained by experiment and by the triangular finite element method [2] and the analytical solution by the *pb*-2 Ritz method [8] are also presented. It can be seen that the results by the present approach agree well with those obtained by the other investigators. The first ten mode shapes of the curved panel are shown in Figure 3. Comparison of the nodal lines of the vibration modes shows that the present results agree qualitatively to those of the *pb*-2 Ritz method [8].

TABLE 1

Convergence of first six non-dimensional frequencies of a square cantilever plate by the DQM

No. of sampling points	Mode					
	1	2	3	4	5	6
7*7	3·4717	8·5104	21·3458	28·4007	30·8654	55·5363
9*9	3·4702	8·5076	21·2914	27·1659	30·9630	54·1861
11*11	3·4705	8·5065	21·2858	27·2007	30·9573	54·2024
13*13	3·4707	8·5061	21·2840	27·1990	30·9550	54·1899
15*15	3·4708	8·5060	21·2836	27·1989	30·9542	54·1863
17*17	3·4709	8·5060	21·2837	27·1988	30·9540	54·1847
19*19	3·4709	8·5061	21·2836	27·1987	30·9539	54·1840
21*21	3·4710	8·5061	21·2837	27·1987	30·9539	54·1837
23*23	3.4710	8·5061	21·2837	27·1987	30·9539	54·1935
Leissa [29]	3·4917	8·5246	21·429	27·331	31·111	54·443

TABLE 2

Natural frequencies (Hz) of the CFFF curved panel (9∗9 sampling points) (E=200 GPa, ρ=7860 kg/m³, ν=0·3, Rs=0·6096 m, h=0·003 m, a=b=0·3048 m)

Method	Mode									
	1	2	3	4	5	6	7	8	9	10
FET†	86·601	139·17	251·30	348·59	393·42	533·37	752·09	746·37	790·10	813·84
Experiment†	85·6	134·5	259	351	395	531	743	751	790	809
pb-2‡	84·406	135·35	244·23	336·45	379·95	521·60	715·19	716·94	759·81	790·71
Present	84·644	136·09	243·07	336·86	380·24	520·22	715·29	717·07	759·52	789·70

† Olson and Lindberg [2].
‡ Lim and Liew [8].

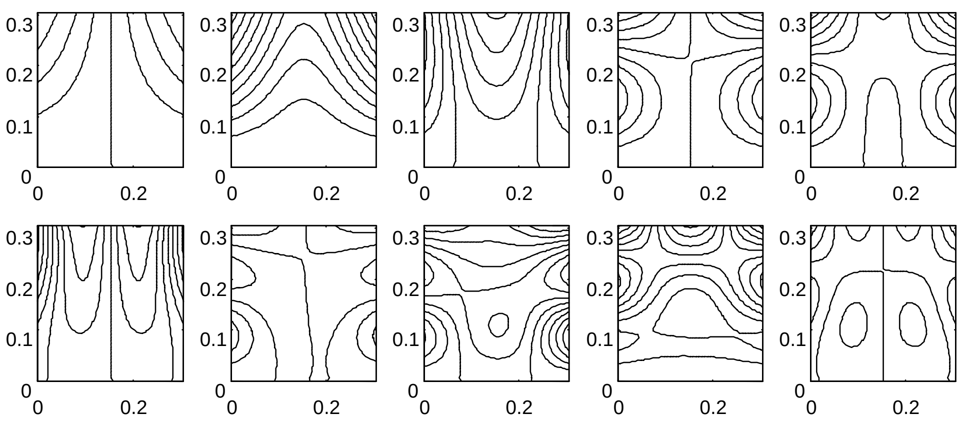

Figure 3. First 10 vibration modes of a cantilever fan blade.

4.2. STUDY 2: EFFECT OF SHALLOWNESS RATIO (R_S/b)

A cantilever curved panel with an aspect ratio $a/b = 1$ is considered. The shallowness ratio (R_S/b) of the panel ranges from 1 to 1000. The first five non-dimensional frequencies are obtained and are shown in Figure 4. As the shallowness ratio increases, the bending and the twisting rigidities decrease such that the natural frequencies decrease, and the natural frequency of the first bending mode decreases more significantly than that of the first twisting mode does. Figure 5 shows the fundamental frequencies versus the shallowness ratio for curved panels with different aspect ratios $a/b = \frac{5}{2}, \frac{3}{2}, 1, \frac{2}{3}$ and $\frac{2}{5}$. It is observed that the fundamental frequencies of curved panels with different aspect ratios exhibit a similar trend that the fundamental frequencies decrease as the shallowness ratio increases.

4.3. STUDY 3: EFFECT OF THICKNESS RATIO (h/b)

The fundamental frequencies of curved panels with $a/b = 1$ and different thickness ratios $h/b = 0{\cdot}005$, 0·01, 0·02 and 0·05 versus the shallowness ratio are plotted in Figure 6. It is observed that the thickness ratio has a significant effect on the non-dimensional fundamental frequency of panels with a small shallowness ratio, say, $R_S/b < 20$, and has no effect for panels with a large shallowness ratio, say, $R_S/b > 100$.

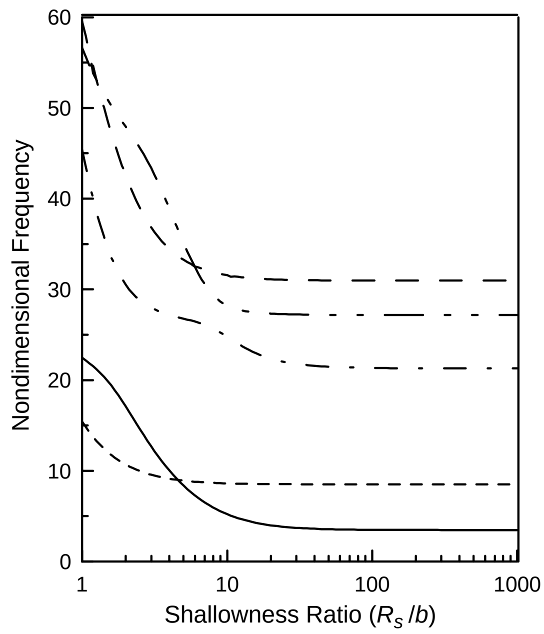

Figure 4. First five non-dimensional frequencies of a cantilever panel versus shallowness ratio ($h/b = 0{\cdot}01$, $a/b = 1$).

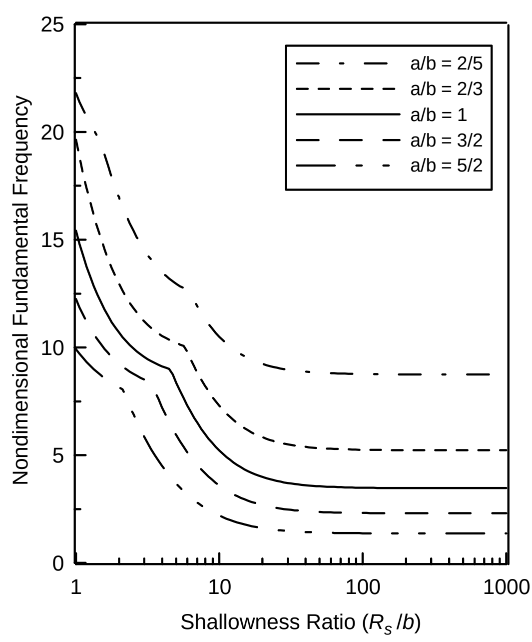

Figure 5. Non-dimensional fundamental frequencies of cantilever curved panels with different aspect ratios.

4.4. STUDY 4: CURVED PANEL WITH VARIABLE CURVATURE

Dynamic behaviors of curved panels with varying curvatures are studied. The panels are parabolic in the chordwise direction, $z = cy^2$, where c is a shape parameter. The first eight non-dimensional natural frequencies of parabolic panels with $c = 0{\cdot}25$ and $0{\cdot}8$ are shown

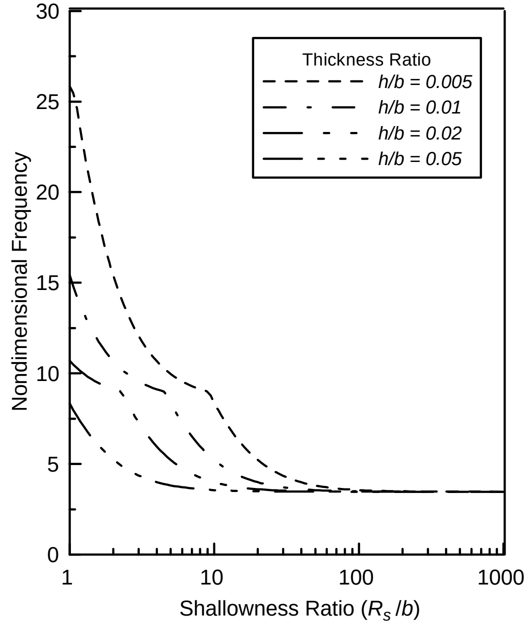

Figure 6. Non-dimensional fundamental frequency of a cantilever curved panel with different thickness ratios.

TABLE 3

First eight non-dimensional natural frequencies of parabolic curved panels, $\varpi = \omega a^2\sqrt{\rho h/D}$ (9∗9 sampling points, a/b=1). Case (a) $z=0{\cdot}25y^2$, b/h=100; Case (b) $z=0{\cdot}8y^2$, b/h=40.

Case	Method	Mode							
		1	2	3	4	5	6	7	8
(a)	DQM	10·507	16·876	30·448	41·695	47·292	65·157	88·852	89·235
	Ritz†	10·500	17·005	30·352	41·869	47·187	64·314	90·097	90·325
(b)	DQM	10·699	17·950	30·757	41·557	46·567	63·414	86·862	87·931
	Ritz†	10·670	17·747	31·130	42·351	44·512	64·890	88·435	88·483

†Wang [6].

in Table 3, together with Wang's results by using the Ritz method [6]. Good agreement between the present and Wang's results is observed.

5. CONCLUSION

Free-vibration characteristics of cantilever non-circular curved panels of rectangular planforms are analyzed by using the DQM. Good convergence trends of the DQM are observed from the vibration analysis of a cantilever curved panel. The effects of shallowness, thickness and aspect ratios on natural frequencies of the panel are investigated. Some conclusions are given as follows:

1. As the shallowness ratio of a cantilever curved panel increases, the bending and the twisting rigidities decrease such that the natural frequencies decreases.

2. The effect of thickness ratio on natural frequencies is more significant for panels with a smaller shallowness ratio than for panels with a larger shallowness ratio.

3. As the aspect ratio of a cantilever curved panel increases, the fundamental frequency decreases.

REFERENCES

1. W. Soedel 1993 *Vibrations of Shells and Plates*. New York: Marcel Dekker, Inc; second edition.
2. M. D. Olson and G. M. Lindberg 1971 *Journal of Sound and Vibration* **19**, 299–318. Dynamic analysis of shallow shell with a doubly curved triangular finite element.
3. A. W. Leissa 1973 *Vibration of Shells*, *NASA SP*-288. Washington, DC: US Government Printing Office.
4. A. W. Leissa, J. K. Lee and A. J. Wang 1981 *Journal of Sound and Vibration* **78**, 311–328. Vibrations of cantilevered shallow cylindrical shells of rectangular planform.
5. A. W. Leissa, J. K. Lee and A. J. Wang 1982 *American Society of Mechanical Engineers Journal of Engineering for Power* **104**, 296–302. Rotating blade vibration analysis using shells.
6. A. J. Wang 1982 *Ph.D. Dissertation, The Ohio State University, Columbus, OH. Vibration analysis of turbomachinery blades by shell theory*. .
7. A. W. Leissa and M. S. Ewing 1983 *American Society of Mechanical Engineers Journal of Engineering for Power* **105**, 383–392. Comparison of beam and shell theories for the vibrations of thin turbomachinery blades.
8. C. W. Lim and K. M. Liew 1994 *Journal of Sound and Vibration* **173**, 343–375. A *pb*-2 Ritz formulation for flexural vibration of shallow cylindrical shells of rectangular planform.
9. K. M. Liew, C. W. Lim and S. Kitipornchai 1997 *Applied Mechanics Reviews* **50**, 431–444. Vibration of shallow shells.
10. R. E. Bellman and J. Casti 1971 *Journal of Mathematical Analysis and Application* **34**, 235–238. Differential quadrature and long-term integration.
11. C. W. Bert, S. K. Jang and A. G. Striz, 1988 *American Institute of Aeronautics and Astronautics Journal* **26**, 612–618. Two new approximate methods for analyzing free vibration of structural components.
12. A. G. Striz, S. K. Jang and C. W. Bert 1988 *Thin-Walled Structures* **6**, 51–62. Nonlinear bending analysis of thin circular plates by differential quadrature.
13. S. K. Jang, C. W. Bert, and A. G. Striz 1989 *International Journal for Numerical Methods in Engineering* **28**, 561–577. Application of differential quadrature to static analysis of structural components.
14. A. N. Sherbourne and M. D. Pandey 1991 *Computers and Structures* **40**, 903–913. Differential quadrature method in the buckling analysis of beams and composite plates.
15. C. Shu and B. E. Richards 1992 *International Journal for Numerical Methods in Fluids* **15**, 791–798. Application of generalized differential quadrature to solve two-dimensional incompressible Navier-Stokes equations.
16. R. H. Gutierrez and P. A. A. Laura 1994 *Journal of Sound and Vibration* **178**, 269–271. Solution of the Helmholtz equation in a parallelogrammic domain with mixed boundary conditions using the differential quadrature method.
17. C. W. Bert and M. Malik 1996 *Applied Mechanics Review* **49**, 1–28. Differential quadrature method in computational mechanics: a review.
18. M. Malik and C. W. Bert 1998 *International Journal of Solids and Structures* **35**, 299–318. Three-dimensional elasticity solutions for free vibrations of rectangular plates by the differential quadrature method.
19. K. M. Liew and T. M. Teo 1999 *Journal of Sound and Vibration* **220**, 577–599. Three-dimensional vibration analysis of rectangular plates based on differential quadrature method.
20. S.-T. Choi, J.-D. Wu and Y.-T. Chou 2000 *American Institute of Aeronautics and Astronautics Journal* **38**, 851–856. Dynamic analysis of a spinning Timoshenko beam by the differential quadrature method.
21. S.-T. Choi and Y.-T. Chou 2001 *Journal of Sound and Vibration* **240**, 937–953. Vibration analysis of elastically supported turbomachinery blades by the modified differential quadrature method.

22. X. WANG and C. W. BERT 1993 *Journal of Sound and Vibration* **162**, 566–572. A new approach in applying differential quadrature to static and free vibrational analyses of beams and plates.
23. C. W. BERT, X. WANG, A. G. STRIZ 1994 *Acta Mechanics* **102**, 11–24. Static and free vibrational analysis of beams and plates by differential quadrature method.
24. M. MALIK and C. W. BERT 1996 *International Journal for Numerical Methods in Engineering* **39**, 1237–1258. Implementing multiple boundary conditions in the DQ solution of higher-order PDE's: application to free vibration of plates.
25. C. SHU and H. DU 1997 *International Journal of Solids and Structures* **34**, 819–835. Implementation of clamped and simply supported boundary conditions in the GDQ free vibration analysis of beams and plates.
26. C. SHU and H. DU 1997 *International Journal of Solids and Structures* **34**, 837–846. A generalized approach for implementing general boundary conditions in the GDQ free vibration analysis of plates.
27. W. CHEN, A. G. STRIZ and C. W. BERT 1997 *International Journal for Numerical Methods in Engineering* **40**, 1941–1956. A new approach to the differential quadrature method for fourth-order equations.
28. S. T. CHOI and Y. T. CHOU 1998 *Proceedings of ASME International Computers in Engineering Conference Atlanta, GA, U.S.A.* Structural analysis by the differential quadrature method using the modified weighting matrices.
29. A. W. LEISSA 1973 *Journal of Sound and Vibration* **31**, 257–293. The free vibration of rectangular plates.

APPENDIX A

Sub-matrices of $[K_G]$ in equation (16) are

$$\bar{K}_{11} = -\bar{W}_X\bar{B}^{(N_{xx})}\bar{K}\bar{W}_X\bar{B}^{(u)} - \mu\bar{W}_S\bar{B}^{(T_{sx})}\bar{K}\bar{W}_S\bar{B}^{(u)},$$

$$\bar{K}_{12} = -\bar{W}_X\bar{B}^{(N_{xx})}\bar{K}v\bar{W}_S\bar{B}^{(v)} - \mu\bar{W}_S\bar{B}^{(T_{sx})}\bar{K}\bar{W}_X\bar{B}^{(v)},$$

$$\bar{K}_{13} = -\bar{W}_X\bar{B}^{(N_{xx})}\bar{K}v\bar{R}_s^{-1},$$

$$\bar{K}_{21} = -\mu\bar{W}_X\bar{B}^{(T_{xs})}\bar{K}\bar{W}_S\bar{B}^{(u)} - \bar{W}_S\bar{B}^{(N_{ss})}\bar{K}v\bar{W}_X\bar{B}^{(u)},$$

$$\begin{aligned}\bar{K}_{22} = &-\mu\bar{W}_X\bar{B}^{(T_{xs})}\bar{K}\bar{W}_X\bar{B}^{(v)} - \mu\bar{W}_X\bar{B}^{(T_{xs})}\bar{R}_s^{-1}\bar{D}\bar{W}_X\bar{B}^{(\beta_s)}\bar{R}_s^{-1} + \mu\bar{W}_X\bar{R}_s^{-1}\bar{D}\bar{W}_X\bar{B}^{(\beta_s)}\bar{R}_s^{-1}\\ &- \bar{W}_S\bar{B}^{(N_{ss})}\bar{K}\bar{W}_S\bar{B}^{(v)} - \bar{R}_s^{-1}\bar{W}_S\bar{B}^{(M_{ss})}\bar{D}\bar{W}_S\bar{B}^{(\beta_s)}\bar{R}_s^{-1} - \mu\bar{R}_s^{-1}\bar{W}_S\bar{B}^{(M_{xs})}\bar{D}\bar{W}_X\bar{B}^{(\beta_s)}\bar{R}_s^{-1},\end{aligned}$$

$$\begin{aligned}\bar{K}_{23} = &\mu\bar{W}_X\bar{B}^{(T_{xs})}\bar{R}_s^{-1}\bar{D}\bar{W}_S\bar{B}^{(\beta_x)}\bar{W}_X\bar{B}^{(w)} + \mu\bar{W}_X\bar{B}^{(T_{xs})}\bar{R}_s^{-1}\bar{D}\bar{W}_X\bar{B}^{(\beta_s)}\bar{W}_S\bar{B}^{(w)}\\ &- \mu\bar{W}_X\bar{R}_s^{-1}\bar{D}\bar{W}_S\bar{B}^{(\beta_x)}\bar{W}_X\bar{B}^{(w)} - \mu\bar{W}_X\bar{R}_s^{-1}\bar{D}\bar{W}_X\bar{B}^{(\beta_s)}\bar{W}_S\bar{B}^{(w)} - \bar{W}_S\bar{B}^{(N_{ss})}\bar{K}\bar{R}_s^{-1}\\ &+ \bar{R}_s^{-1}\bar{W}_S\bar{B}^{(M_{ss})}\bar{D}\bar{W}_S\bar{B}^{(\beta_s)}\bar{W}_S\bar{B}^{(w)} + \bar{R}_s^{-1}\bar{W}_S\bar{B}^{(M_{ss})}\bar{D}v\bar{W}_X\bar{B}^{(\beta_x)}\bar{W}_X\bar{B}^{(w)}\\ &+ \mu\bar{R}_s^{-1}\bar{W}_X\bar{B}^{(M_{xs})}\bar{D}\bar{W}_S\bar{B}^{(\beta_x)}\bar{W}_X\bar{B}^{(w)} + \mu\bar{R}_s^{-1}\bar{W}_X\bar{B}^{(M_{ss})}\bar{D}\bar{W}_X\bar{B}^{(\beta_s)}\bar{W}_S\bar{B}^{(w)},\end{aligned}$$

$$\bar{K}_{31} = \bar{R}_s^{-1}\bar{K}v\bar{W}_X\bar{B}^{(u)},$$

$$\begin{aligned}\bar{K}_{32} = &-\bar{W}_X\bar{B}^{(V_{xz})}\bar{W}_X\bar{B}^{(M_{xx})}\bar{D}v\bar{W}_S\bar{B}^{(\beta_s)}\bar{R}_s^{-1} - \bar{W}_X\bar{B}^{(V_{xz})}\bar{W}_X\bar{B}^{(M_{xx})}\bar{D}(1-v)\bar{W}_X\bar{B}^{(\beta_s)}\bar{R}_s^{-1}\\ &+ \mu\bar{W}_X\bar{W}_S\bar{B}^{(M_{xs})}\bar{D}\bar{W}_X\bar{B}^{(\beta_s)}\bar{R}_s^{-1} - \bar{W}_S\bar{B}^{(V_{sz})}\bar{W}_X\bar{B}^{(M_{xs})}\bar{D}(1-v)\bar{W}_S\bar{B}^{(\beta_s)}\bar{R}_s^{-1}\\ &- \bar{W}_S\bar{B}^{(V_{sz})}\bar{W}_S\bar{B}^{(M_{ss})}\bar{D}\bar{W}_S\bar{B}^{(\beta_s)}\bar{R}_s^{-1} + \mu\bar{W}_S\bar{W}_X\bar{B}^{(M_{sx})}\bar{D}\bar{W}_X\bar{B}^{(\beta_s)}\bar{R}_s^{-1} + \bar{R}_s^{-1}\bar{K}\bar{W}_S\bar{B}^{(v)},\end{aligned}$$

$$
\begin{aligned}
\bar{K}_{33} = {} & \bar{W}_X \bar{B}^{(V_{xz})} \bar{W}_X \bar{B}^{(M_{xx})} \bar{D} \bar{W}_X \bar{B}^{(\beta_x)} \bar{W}_X \bar{B}^{(w)} + \bar{W}_X \bar{B}^{(V_{xz})} \bar{W}_X \bar{B}^{(M_{xx})} \bar{D} v \bar{W}_S \bar{B}^{(\beta_s)} \bar{W}_S \bar{B}^{(w)} \\
& + \bar{W}_X \bar{B}^{(V_{xz})} \bar{W}_S \bar{B}^{(M_{sx})} \bar{D}(1-v) \bar{W}_S \bar{B}^{(\beta_x)} \bar{W}_X \bar{B}^{(w)} + \bar{W}_X \bar{B}^{(V_{xz})} \bar{W}_S \bar{B}^{(M_{xx})} \bar{D}(1-v) \bar{W}_X \bar{B}^{(\beta_s)} \bar{W}_S \bar{B}^{(w)} \\
& - \mu \bar{W}_X \bar{W}_S \bar{B}^{(M_{xs})} \bar{D} \bar{W}_S \bar{B}^{(\beta_x)} \bar{W}_X \bar{B}^{(w)} - \mu \bar{W}_X \bar{W}_S \bar{B}^{(M_{xs})} \bar{D} \bar{W}_X \bar{B}^{(\beta_s)} \bar{W}_S \bar{B}^{(w)} \\
& + \bar{W}_S \bar{B}^{(V_{sz})} \bar{W}_X \bar{B}^{(M_{xs})} \bar{D}(1-v) \bar{W}_S \bar{B}^{(\beta_x)} \bar{W}_X \bar{B}^{(w)} + \bar{W}_S \bar{B}^{(V_{sz})} \bar{W}_X \bar{B}^{(M_{xs})} \bar{D}(1-v) \bar{W}_X \bar{B}^{(\beta_s)} \bar{W}_S \bar{B}^{(w)} \\
& + \bar{W}_S \bar{B}^{(V_{sz})} \bar{W}_S \bar{B}^{(M_{ss})} \bar{D} \bar{W}_S \bar{B}^{(\beta_s)} \bar{W}_S \bar{B}^{(w)} + \bar{W}_S \bar{B}^{(V_{sz})} \bar{W}_S \bar{B}^{(M_{ss})} \bar{D} v \bar{W}_X \bar{B}^{(\beta_x)} \bar{W}_X \bar{B}^{(w)} \\
& - \mu \bar{W}_S \bar{W}_X \bar{B}^{(M_{sx})} \bar{D} \bar{W}_S \bar{B}^{(\beta_x)} \bar{W}_X \bar{B}^{(w)} - \mu \bar{W}_S \bar{W}_X \bar{B}^{(M_{sx})} \bar{D} \bar{W}_X \bar{B}^{(\beta_s)} \bar{W}_S \bar{B}^{(w)} + \bar{R}_s^{-1} \bar{K} \bar{R}_s^{-1},
\end{aligned}
$$

where $\mu = (1-v)/2$.

Sub-matrices of $[M_G]$ in equation (16) are

$$\bar{\bar{M}}_{11} = \bar{\bar{M}}_{22} = \bar{\bar{M}}_{33} = \rho \bar{H}.$$